3.3 Rauschinduzierte raum-zeitliche Muster

Raum-zeitliche Systeme: anregbare Medien

→ raum-zeitliche Oszillationen und Wellen können auch durch Rauschen induziert werden.

Sagués, Sancho, García-Ojalvo: Rev. Mod. Phys. 79, 829 (2007)
García-Ojalvo et al: PRL 71, 1542 (1993)
Kadar, Wang, Showalter: Nature 391, 770 (1998) (Wellen)
Schöll, in Nonlinear Dyn. of Nanosystems (eds. Radons et al) (Wiley 2010)

1. Rauschinduzierte Fronten in Halbleiter-Übergitter

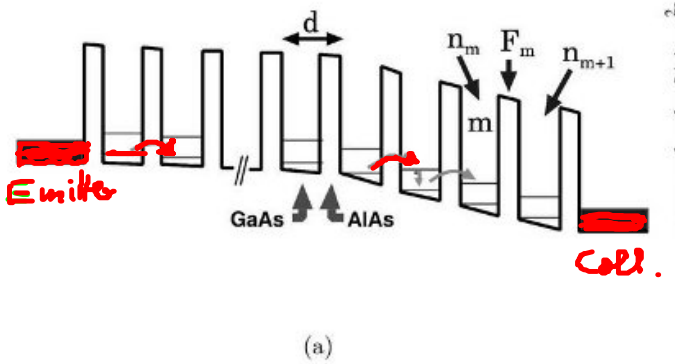

(a) (b)

FIG. 1 (a) Superlattice energy band structure of alternating GaAs and AlAs layers under bias. (b) Current density vs electric field characteristic at the emitter barrier (straight line) and between two neutral wells exhibiting negative differential conductivity.

Hizanidis, Balanov, Amann, Schöll, Int. J. Bif. Chaos 16, 1701 (2006)

$$\varepsilon_r \varepsilon_0 (F_m - F_{m-1}) = e(n_m - N_D)$$

$m = 1, \ldots, N$
diskretes Raum-Gerät
($e<0$, Feld $F_m < 0$, Dotierungsdichte N_D, El. konz. n_m)

$$e\dot{n}_m = J_{m-1\to m} + D\xi_m(t) - J_{m\to m+1} - D\xi_{m+1}(t)$$

Ladungsträger-Kontinuitäts-Gl. mit Gauß'schem weißen Rauschen $\langle \xi_m(t) \rangle = 0$

$$\langle \xi_m(t)\, \xi_{m'}(t') \rangle = \delta(t-t')\, \delta_{mm'},$$

Schrotrauschen (shot noise), therm. Rauschen

resonante Tunnelstromdichte $J_{n \to n+1}(F_n, n_n, n_{n+1})$ nichtlinear

Anwendung: Hochfrequenzoszillator (GHz)

Heinrich et al: New J. Phys. (Nov. 2010): Netzwerk von Tunneldioden

Hizanidis, Balanov, Amann, Schöll: PRL 96, 244104 (2006): verschiedene Fronten

$D = 0$: stationäre Felddomänen → laufende Domänen

SNIPER-Bif. (wie gener. Modell in §3.2)

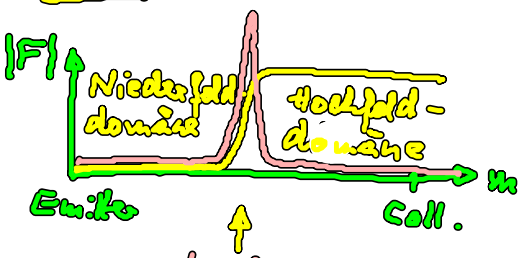

Ladungsanreicherungsfront

globale Bedingung: $U = -\sum_{n=0}^{N} F_n d$

Ohm'sche Randbed. am Emitterkontakt: $J_{0 \to 1} = \sigma F_0$ (Kontakthalbleitf. σ)

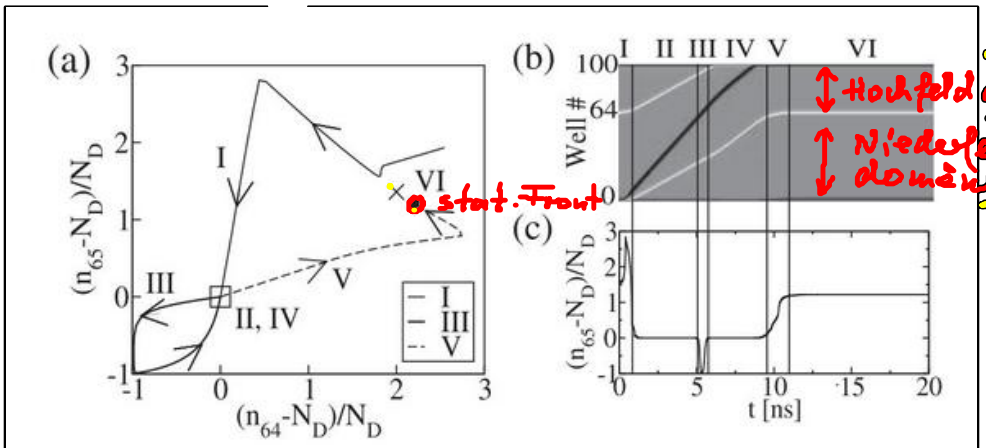

Hizanidis, PRL

FIG. 4. (a) Phase portrait in terms of electron densities n_{65} and n_{64}, normalized to the donor density N_D, below the global bifurcation. (b) Space-time plot and (c) time series of n_{65} for the trajectory shown in (a). The different parts of the trajectory are labeled by roman numerals I–VI in (a), (b), and (c). Parameters as in Fig. 1, $D = 0$.

$D \neq 0$: rauschinduzierte Domänenbewegung (laufende Front)

Kohärenzresonanz

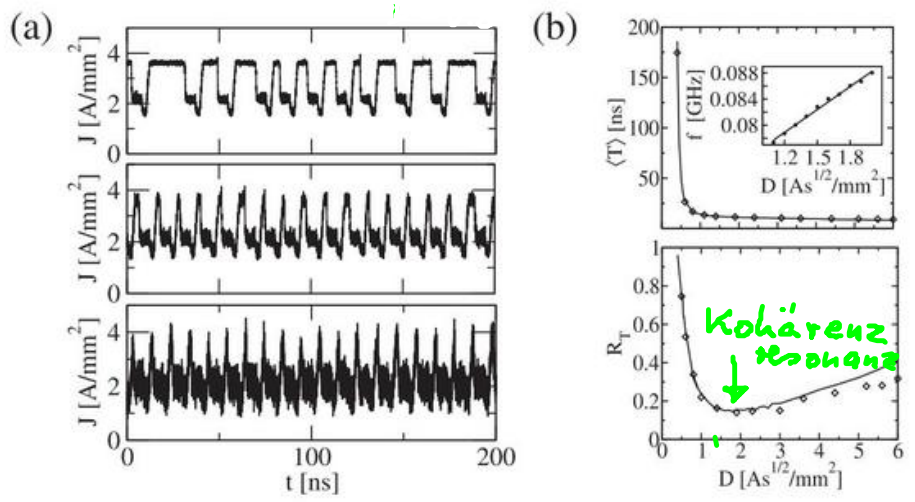

FIG. 2. (a) Three noise realizations of the current density $J(t)$. From top to bottom, $D = 0.8$, $D = 2.0$, and $D = 5.0$ A $s^{1/2}/m^2$. (b) Mean interspike interval (top panel) and its normalized fluctuations R_T (bottom panel) versus noise intensity. Lines, constant D; diamonds, $D \sim J_{m-1\to m}^{1/2}$ [18]. The inset shows the peak frequency versus D.

mittlere ISI

Maß für Kohärenz:
R_T = Standardabweichung der Interspike-Intervalle (ISI)

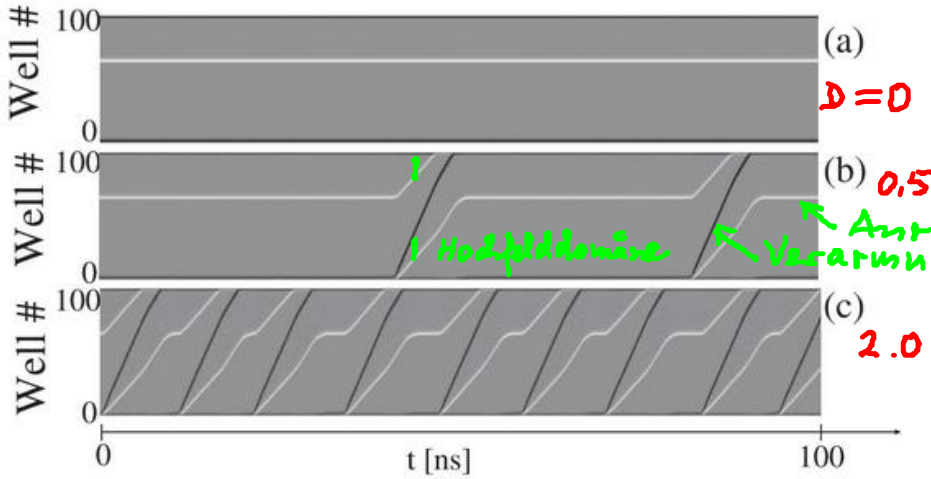

← Anreicherungsfront

optimale Kohärenz

↓

Kohärenzresonanz

FIG. 1. Noise-induced front motion: Space-time plots of the electron density for (a) $D = 0$ (no noise), (b) $D = 0.5$ A s$^{1/2}$/m^2, and (c) $D = 2.0$ A s$^{1/2}$/m^2. Light and dark shading corresponds to electron accumulation and depletion fronts, respectively. The emitter is at the bottom. Parameters: $U = 2.99$ V, $\sigma = 2.082\,101\,248\,8\ \Omega^{-1}\,\mathrm{m}^{-1}$, $N_D = 10^{11}$ cm^{-2}, $T = 20$ K, $N = 100$ GaAs wells of width $w = 8$ nm, and $Al_{0.3}Ga_{0.7}As$ barriers of width $b = 5$ nm, energies $E^a = 41.5$ meV, $E^b = 160$ meV, scattering width $\Gamma = 8$ meV, transition matrix elements $H^{a,b}_{m,m+1} = -eF_m \times 0.0127$ m, $H^{a,a}_{m+1,m} = -0.688$ meV, $H^{b,b}_{m+1,m} = 1.263$ meV, as in Ref. [9].

2. Resonante Tunneldiode

Stegemann, Balanov, Schöll: PRE 71, 016221 (2005)
PRE 73, 016203 (2006)

Majer, Schöll: PRE 79, 011109 (2009)

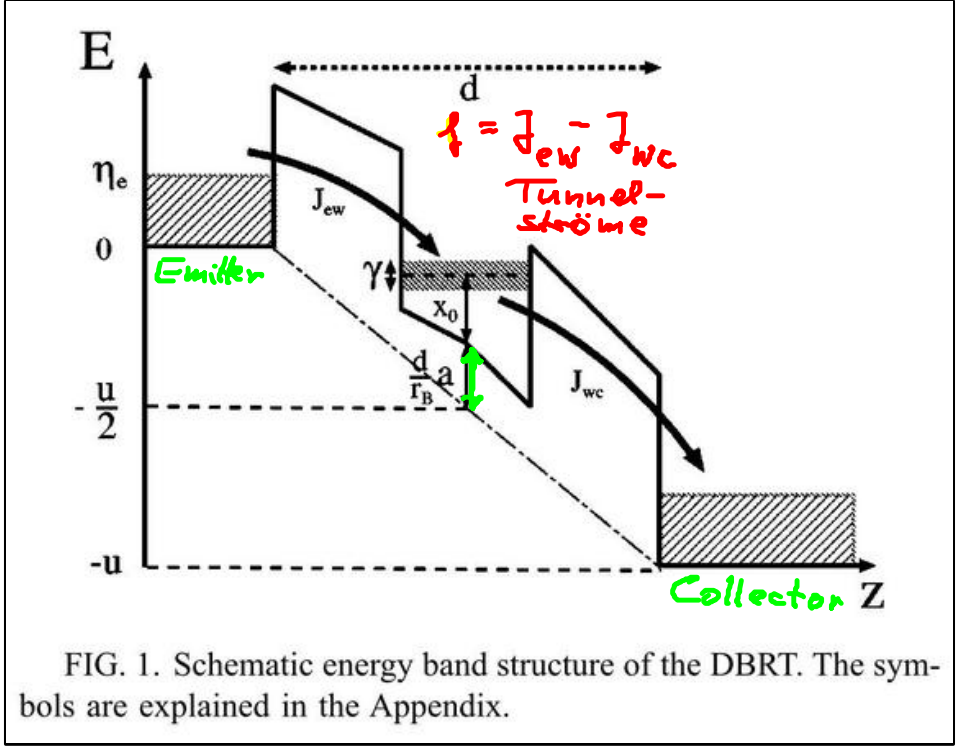

FIG. 1. Schematic energy band structure of the DBRT. The symbols are explained in the Appendix.

$J = J_{ew} - J_{wc}$
Tunnel-ströme

Unterbach, PRE (2003)

Bandverbiegung durch Ladungsansammlung im Quantentopf (QW)

⇒ Z-förmige N-förmige I-U-Char.

$$\dot{a} = f(a,u) + D\frac{d}{dx^2}a + D_a\xi(x,t)$$

$$\dot{u} = \frac{1}{\varepsilon}(U_0 - u - RJ) + D_u\xi(t)$$

Ladungsdichte a (dim. los)

Kirchhoff-Gl., $\varepsilon = \frac{RC}{\tau_a}$

Reaktions-Diff.-Modell mit globaler Kopplung $J = \frac{1}{L}\int_0^L dx\, j(x)$ (x ... lokal)

$U_0 = u + RI$

$I = J + C\dot{u}$

- raum-zeitl. Dgl. (breathing current filament)

durch Hopf-Bif. ($D = 0$)

• knapp unterhalb der Hopf-Bif.: rauschinduziertes Atmen (D ≠ 0) (breathing)

⇓

keine Kohärenzresonanz

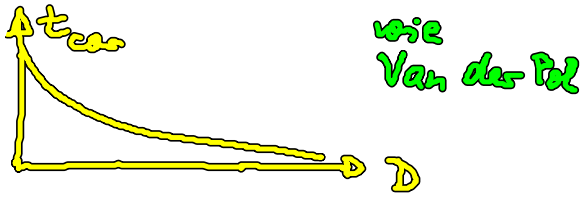

wie Van der Pol

Stefanovska (2005)

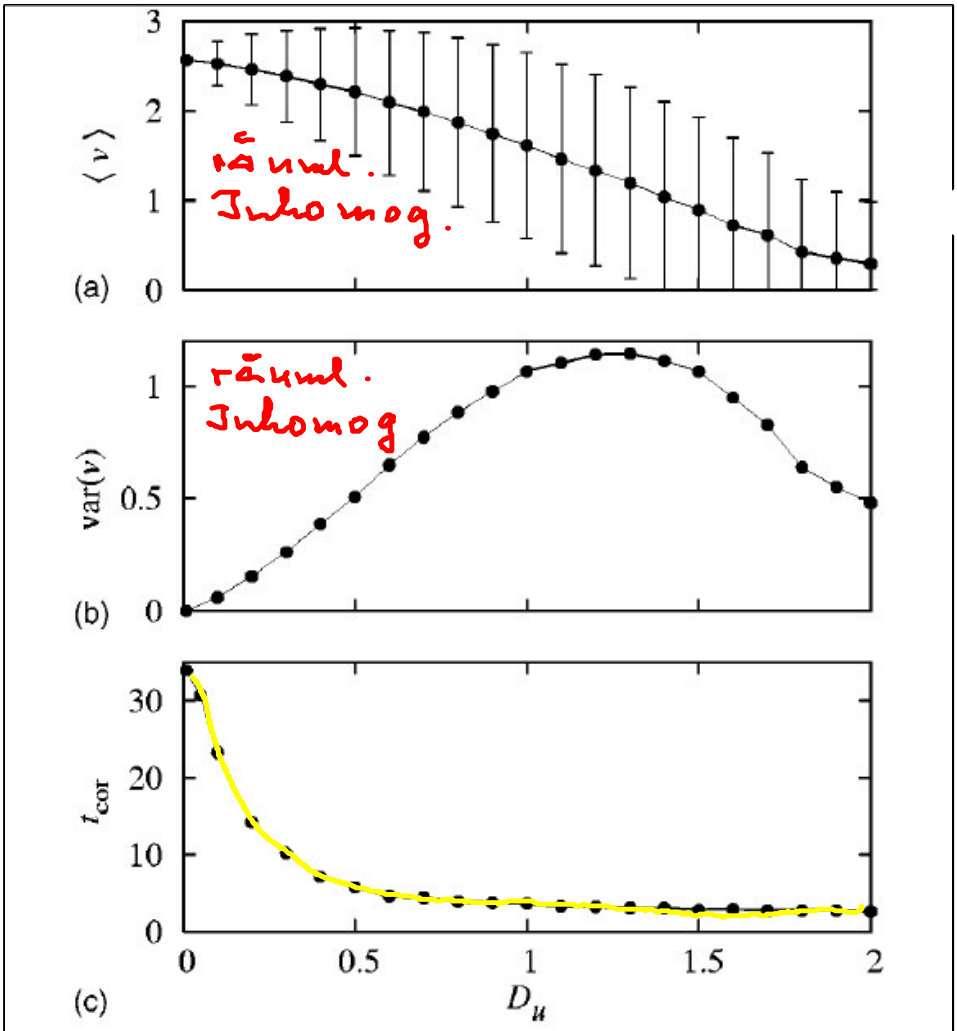

FIG. 8. Spatial and temporal ordering of the dynamics in dependence on the noise intensity D_u. (a) Time average of the order parameter $v(t)$ defined in Eq. (3); error bars correspond to the standard deviation. (b) Variance of the parameter v [corresponding to the square of the error bars from (a)]. (c) Correlation time [Eq. (4)].

Majer (2009)

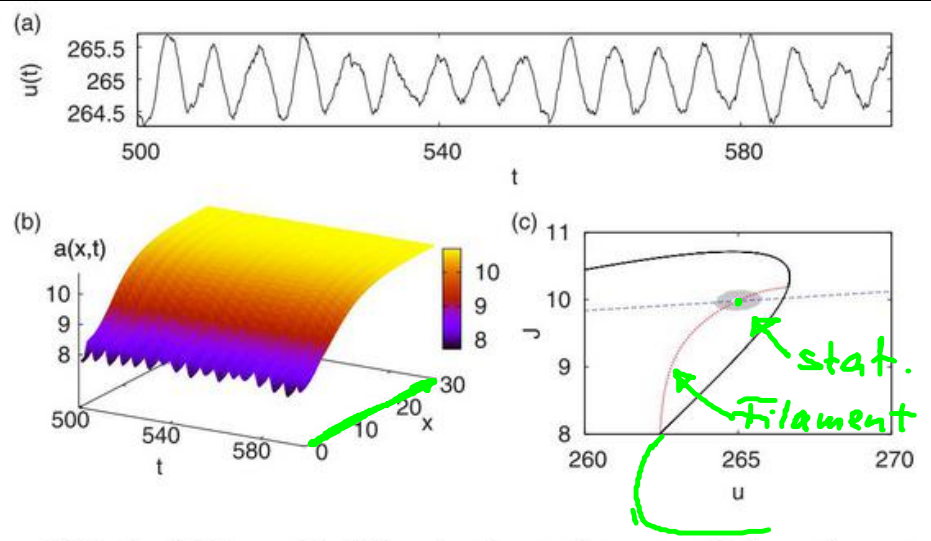

FIG. 1. (Color online) Stochastic spatiotemporal dynamics under multiple time-delayed feedback control. (a) Voltage time series $u(t)$ (in units of 0.35 mV), (b) charge carrier density $a(x,t)$ (in units of $10^{10}/\mathrm{cm}^2$), (c) phase portrait of current J (in units of 500 A/cm^2) vs voltage u. Space x and time t are scaled in units of 100 nm and 3.3 ps, respectively, corresponding to typical device parameters at 4 K [29]. Parameters are $U_0=-84.2895$, $r=-35$, $\varepsilon=6.2$, $D_u=0.1$, $D_a=10^{-4}$, $K=0.1$, $\tau=6.3$, $R=0.5$.

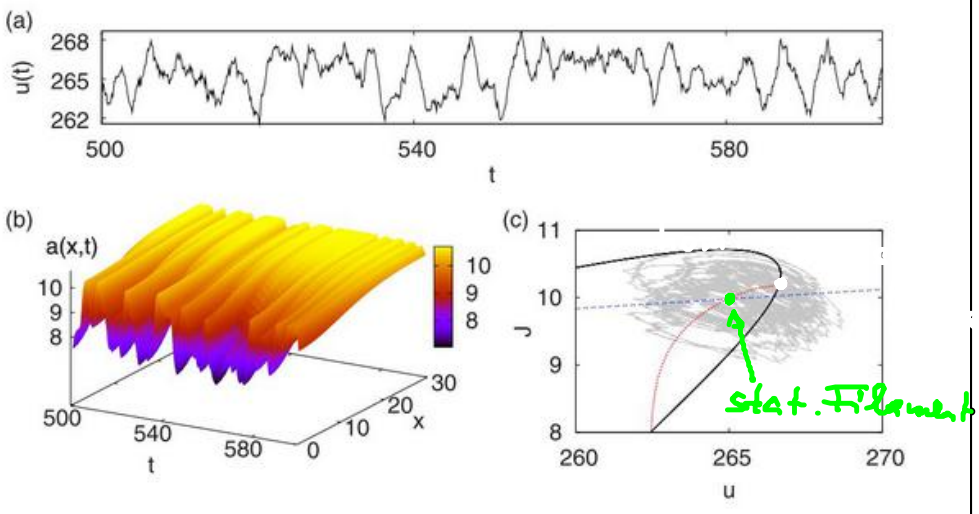

FIG. 2. (Color online) Same as Fig. 1 for $D_u=1.0$.

mehr Rauschen
→ zeitlich irregulärer
→ räumlich homogener